The 7th International Supercritical CO_2 Power Cycles Symposium
February 21 – 24, 2022, San Antonio, Texas
Paper #182

Hydraulic development length and boundary condition effects on local sCO_2 heat transfer coefficients

Yang Chao
Ph.D. Candidate
Embry-Riddle Aeronautical University
Daytona Beach, Florida

Nicholas C. Lopes
Masters Student
Embry-Riddle Aeronautical University
Daytona Beach, Florida

Mark A. Ricklick
Associate Professor
Embry-Riddle Aeronautical University
Daytona Beach, Florida

Sandra K.S. Boetcher
Professor
Embry-Riddle Aeronautical University
Daytona Beach, Florida

ABSTRACT

Recent numerical studies on heat transfer in sCO_2 pipe flows have settled upon a domain consisting of a fixed-length adiabatic section prior to a heat-transfer region. It is assumed the entrance length, which is represented by the total length of the adiabatic section, is long enough to generate hydraulically fully developed flow, such that the influence of the entrance is eliminated. However, the criteria used in subcritical flows may not be appropriate for supercritical fluids and may vary from the perspective of velocity profile and local heat transfer coefficient. Boundary conditions including mass flux, heat flux, and inlet temperature are varied to investigate their effects on the development length. Many of these single-pipe numerical studies are also conducted with either a constant heat flux or constant temperature boundary condition. These are often treated as simplifications or adequate substitutions of double-pipe heat exchangers involving a conjugate boundary condition, which are common in the experimental literature. Very few investigations have acknowledged the potential discrepancies in heat transfer behavior between the constant heat flux or temperature single-pipe boundary condition and that of a conjugate double-pipe heat exchanger. This work seeks to evaluate the hydraulic entrance length criteria for numerical sCO_2 pipe flow and to demonstrate that the constant heat flux or temperature boundary conditions for sCO_2 single-pipe flow are not appropriate simplifications of a double-pipe heat exchanger with a conjugate boundary condition.

INTRODUCTION

The heat transfer coefficient of supercritical CO_2 (sCO_2) pipe flow has been investigated numerically by various researchers. The most widely used numerical model is a straight pipe, consisting of a fixed length of adiabatic section prior to a heat transfer region. The purpose of the adiabatic section is to reduce the entrance effect and ensure the flow is hydraulically fully developed. However, in many papers published in recent years, the authors did not mention how the adiabatic length was determined, nor did they provide an analysis of the suitability of

the chosen entrance length. In some textbooks, it is mentioned that the entrance region length is about 10 to 60 times of diameter [1-2], but it is not known if supercritical CO_2 can be applied to this criterion. In 2004, Dang and Hihara [3] performed an experiment of sCO_2 cooled by water in a counterflow double-pipe heat exchanger, which is adopted by many researchers as the experimental data for validating their single-pipe numerical results. In their experimental paper, the length of adiabatic section was not mentioned. Many subsequent researchers who validate against Dang and Hihaha's data either outright neglect to mention their own adiabatic length, or simply assume a length, which is generally 200mm. Most assume this adiabatic length is long enough after comparing their heat transfer coefficients to the experimental data. In order to evaluate the effect of different adiabatic length, different numerical models with various adiabatic lengths prior to a consistent 500mm heat transfer region were tested.

Additionally, single-pipe sCO_2 studies [4-6] conducted with constant heat flux (or to a lesser extent constant temperature) boundary conditions are often validated against the experimental results of double-pipe heat exchangers, of which Dang and Hihara [3] is a primary reference. In several cases, the averaged heat flux found from a double-pipe heat exchanger experiment is used as the constant heat flux boundary condition for a single-pipe simulation. In their experiment, Dang and Hihara [3] reported only average wall heat fluxes for their iterations and assumed these to be constant throughout the length of their test section. However, the nature of a counterflow double-pipe heat exchanger does not allow this to be a valid assumption. An inherent, non-uniform, conjugate boundary condition in their double-pipe heat exchanger will always be present between the sCO_2, whose heat transfer properties are subject to high variations under very small temperature changes, and H_2O flows. This will be true even with, for example, a variable H_2O inlet temperature (which they made no mention of) in attempt to maintain a target wall heat flux. It is also worth noting that non-uniformity may be caused by lateral conduction through their copper pipe, especially near regions where the bulk sCO_2 temperatures approach the pseudocritical temperature [7]. As such, simplifying a double-pipe heat exchanger to a single-pipe with a constant boundary condition and validating against the original experiment should be investigated. It is well known that subcritical, turbulent flows are insensitive to the thermal boundary condition. However, due to the strong dependency of sCO_2 heat transfer to the fluid properties, this may not be the case under supercritical conditions. To illustrate this, three numerical models (a single-pipe, single-pipe with a wall, and a double-pipe heat exchanger) were constructed and local heat transfer trends were observed.

NUMERICAL MODELS

Simulation Setup

The real gas properties (RGP) table which includes the thermophysical properties of specific heat, thermal conductivity, density and viscosity was implemented for the numerical analysis. The fluid properties given in RGP tables were imported from the NIST REFPROP Version 9.1 [8] database, which employs the equations of state presented by Span and Wagner [9]. The RGP table covers the ranges of 290–330 K and 3.6–11.6 MPa for temperature and pressure, respectively for all cases. For this study, the temperature range was 10°C to 60°C, the pressure range was 7.999MPa to 8.001 MPa and the resolution of the RGP table was 1000 x 1000. The Shear Stress Transport (SST) k-ω turbulence model was used, with gravity turned on. Mesh independence was achieved for the single pipe and double-pipe heat exchanger, as shown in Figure 1.

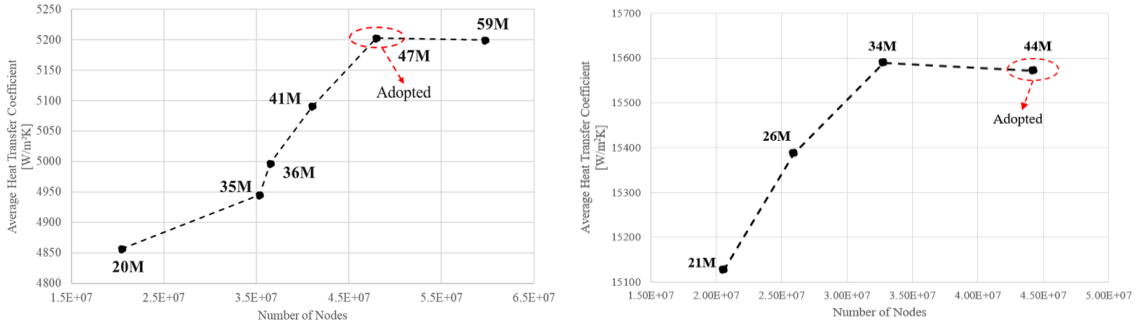

Figure 1. Results of mesh independence studies for the single pipe (left) and double-pipe HX (right).

Development Length Study

The physical geometry of the circular straight pipe is shown in Figure 1a. The diameter is fixed at 6mm, and it consists of three sections: adiabatic entrance with varying length, heat transfer region with different boundary conditions and fixed-length adiabatic outlet. The purpose of the adiabatic outlet is to decrease the effect of the outlet boundary. Constant mass flux inlet and pressure outlet boundary conditions are applied at inlet and outlet of the pipe, respectively. A constant heat flux boundary condition was applied while studying entrance length effects. The testing details for numerical model are shown in Table 1.

Boundary Condition Study

Three geometries were used to compare boundary conditions effects on local heat transfer of sCO_2. As previously discussed, Figure 2a shows a single pipe with an adiabatic entrance, 500mm test section, and an adiabatic outlet of 200mm. Unlike in the development length study, a length of 200mm was selected for examining boundary condition effects in order to remain consistent with the majority of the available literature. In two separate cases (2 and 4 in Table 2), a constant heat flux and constant temperature boundary condition were applied to the geometry in Figure 2a. Figure 2b shows a single pipe with the same geometrical parameters as Figure 2a, but with a 1mm thick copper wall. Again, in two separate cases (3 and 5 in Table 2), a constant heat flux and constant temperature boundary condition were applied to the outer surface of the wall. Figure 2c shows an idealized counterflow double-pipe heat exchanger with sCO_2 flowing through the inner pipe being conjugately cooled by H_2O flowing through a 2mm passage in the opposite direction. This is identical to the experimental setup of Dang and Hihara [3], except for the H_2O entrance and exit, which occurred at 90° to the sCO_2 flow passage in their experiment. The domain consists of 200mm adiabatic regions on either side of the 500mm test section. The sCO_2 and H_2O fluid regions are only interacting through an intermediate copper wall spanning the 500mm test section. The boundary conditions for the double-pipe heat exchanger (case 1) are shown in Table 2. The constant heat flux and constant temperature boundary conditions applied to cases 2-5 are the average values taken from the results of the conjugate problem (case 1). For example, the constant heat flux of 24,455 W/m^2 applied to the single pipe (case 2) was the area-weighted average heat flux found on the sCO_2 side of the conjugate problem (case 1). This encapsulates the process taken by several authors to validate their single-pipe models against a double-pipe heat exchanger experiment.

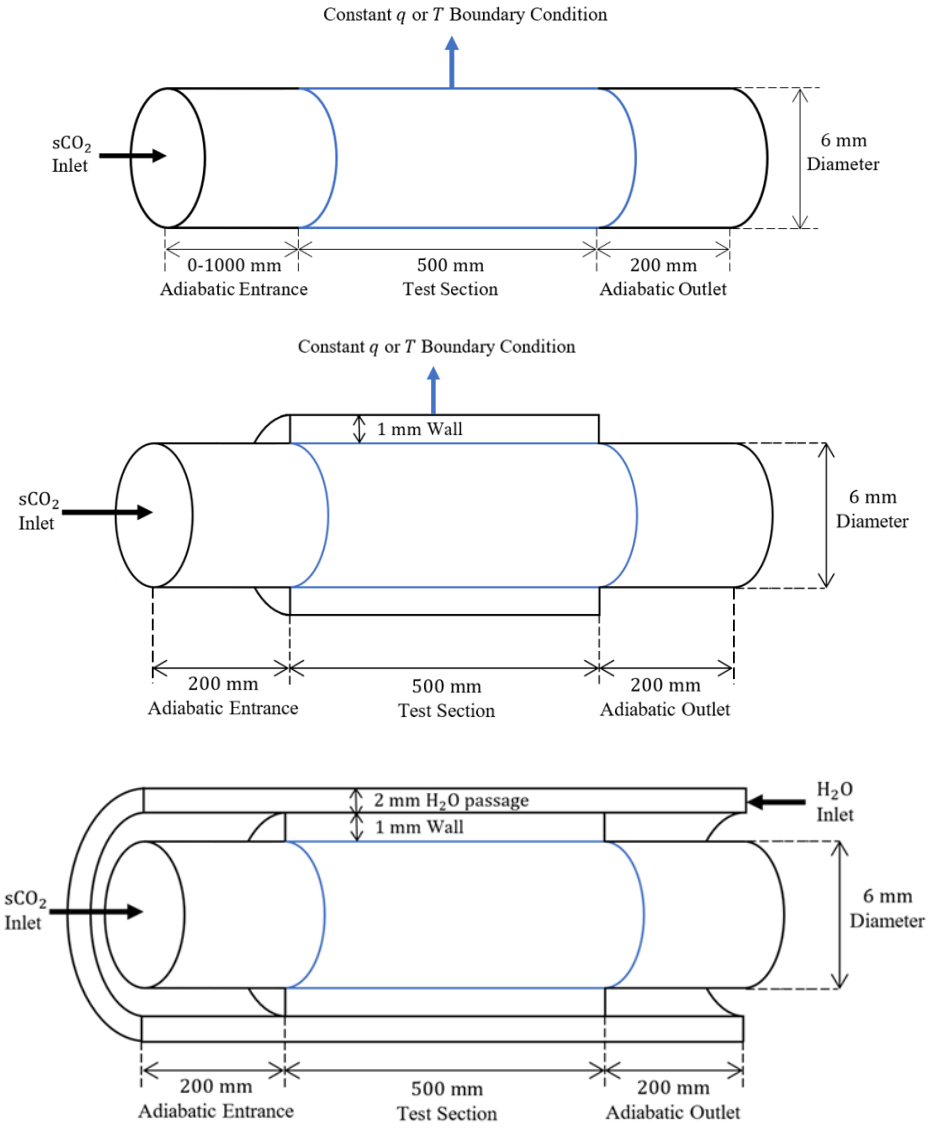

Figure 2. (a) Single-pipe, (b) single-pipe with a wall, and (c) counterflow double-pipe heat exchanger.

Table 1
Testing conditions for development length study.

Adiabatic entrance length (mm)	Mass flux (kg/m²s)	Heat flux (kW/m²)	Inlet Temperature (°C)	Operating Pressure (MPa)
200	200	12	36	8
300	200	12	36	8
400	200	12	36	8
1000	200	12	36	8

Table 2
Testing conditions for boundary condition study. Operating Pressure is 8 MPa.

Case	Geometry	sCO_2 Inlet Temp (°C)	sCO_2 Mass flux (kg/m²s)	H_2O Inlet Temp (°C)	H_2O Mass flux (kg/m²s)	Thermal BC Type	Applied Thermal BC
1	Double-pipe HX	36	200	14	200	Conjugate	--
2	Single pipe	36	200	--	--	Constant heat flux	24,455 W/m^2
4	Single pipe + wall	36	200	--	--	Constant heat flux	18,341 W/m^2
3	Single pipe	36	200	--	--	Constant temperature	29.533 ℃
5	Single pipe + wall	36	200	--	--	Constant temperature	29.478 ℃

RESULTS AND DISCUSSION

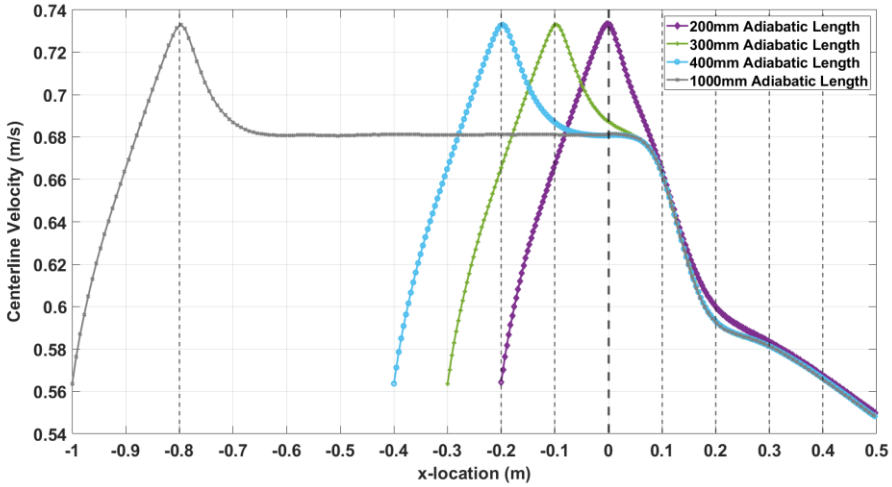

Figure 3. Centerline velocity when inlet temperature is 36°C, Operating pressure is 8 MPa.

Figure 3 shows the centerline velocity for four different adiabatic entrance lengths when inlet temperature is 36°C, which is close to the critical temperature(31.1°C). The x axis is modified to show that for all cases, cooling starts at x=0 location. As shown in the figure, for all four cases, the centerline velocity first increase to a peak value, then decrease, as is common in the development of turbulent flow, because turbulent mixing relaxes the velocity profile. During the cooling process, heat is removed from the flow, the centerline velocity monotonically decreases due to the variation in the fluid properties. However, when the adiabatic entrance length is 200mm, the centerline velocity keeps decreasing with a large slope, until around x=0.2m, the slope gets smaller where the rate of centerline velocity decay is reduced. When the adiabatic entrance length is longer than 200mm, there exists a “shoulder” in the centerline velocity curves around x= 0.05m, where all the centerline velocity curves converge to a single one then continues decreasing consistently. When adiabatic entrance length is longer than 300mm, the centerline velocity curves decrease after the peak value to a constant value about 0.68m/s until they reach the “shoulder”, then start decreasing. It is noticeable that centerline velocity for 200mm adiabatic entrance length doesn’t converge to other curves at the “shoulder” value but meets other curves around x=0.1m, then separates from them. This result shows that when the adiabatic entrance is long enough, the corresponding centerline velocity will converge to one single curve at the “shoulder” value, for this case is x=0.05m and does not separate after that. By using this rule, it also shows that the adiabatic entrance length of 200mm is not long enough for the testing geometry.

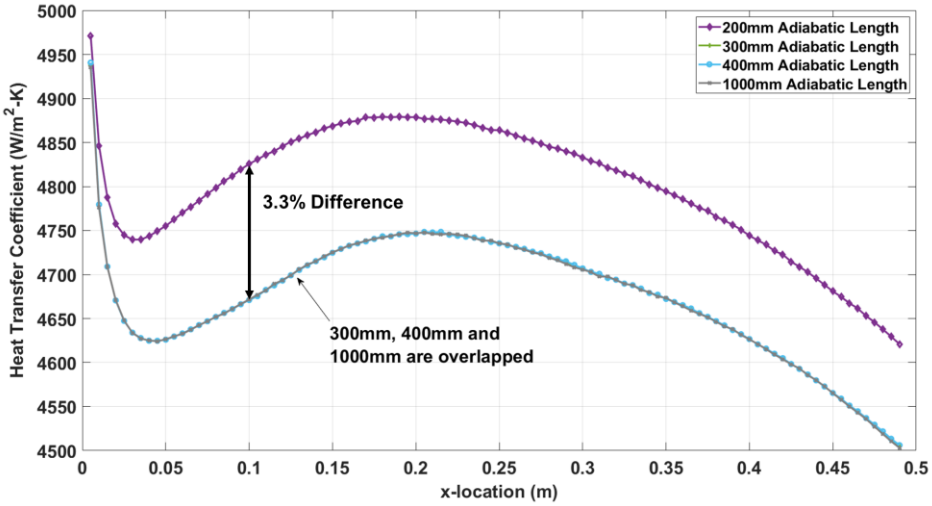

Figure 4. Heat transfer coefficients when inlet temperature is 36°C, Operating pressure is 8MPa.

Figure 4 shows the heat transfer coefficients for these four cases when inlet temperature is 36°C, operating pressure is 8MPa. The x=0 location is where the cooling starts for all cases. The top single curve is when the adiabatic entrance length is 200mm, the bottom three curves are on top of each other, which represent the cases when adiabatic entrance lengths are 300mm, 400mm and 1000mm. As shown in the figure, there is an obvious difference between the top curve and the bottom ones, with a difference of 3.3%. This result also shows that when the adiabatic entrance is long enough, the corresponding heat transfer coefficient are essentially identical. By using this rule, it can be conjectured again that the 200mm adiabatic entrance length is not sufficient to eliminate the entrance length effects from the results.

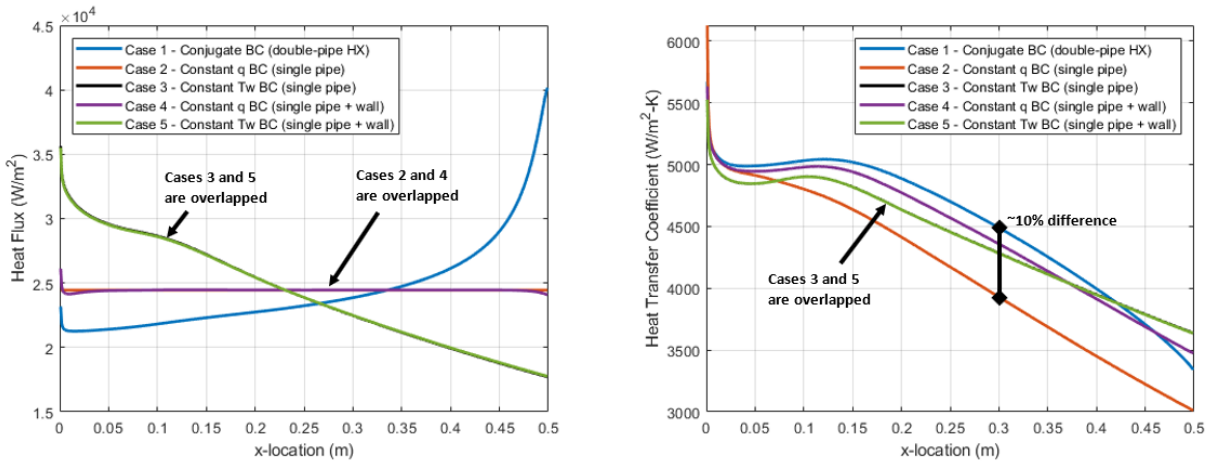

Figure 5. Effect of boundary conditions on heat flux (left) and heat transfer coefficient (right). Cooling starts at x = 0 m. Operating pressure is 8 MPa.

The left plot in Figure 5 compares the effect of the five selected boundary conditions (see Table 2) on local heat flux. As expected, the local heat flux trends of the constant heat flux boundary conditions applied to the single pipe with and without the presence of the wall (cases 2 and 4, respectively) overlap with one another. Similarly, the local heat flux trends of the constant temperature boundary conditions applied to the single pipe with and without the

presence of the wall (cases 3 and 5, respectively) overlap with one another. As expected, the local heat flux trend of the conjugate case (case 1) is not at all like those of the constant heat flux or temperature boundary conditions, despite the boundary conditions of cases 2-5 being set to match the average corresponding values from the conjugate case. The right plot in Figure 5 compares the effect of the five selected boundary conditions (see Table 2) on local heat transfer coefficients. Interestingly, the local heat transfer coefficient trend of case 2, the scenario most often validated against a conjugate model, is the most dissimilar (in terms of magnitude) to the local heat transfer coefficient trend of the conjugate case itself. Inspection of the data reveals that for x = 0.15-0.45m, the percent difference in heat transfer coefficients of these two cases is approximately 10%. A much better comparison could be made between the conjugate model and the single pipe with a heat flux applied on the outer wall, however this is rarely applied in the literature.

CONCLUSIONS

1. Although the impact is small, an entrance length less than 300mm leads to a sensitivity to the hydraulic development length. This is important when attempting to validate results and predict the performance of a heat exchanger design.
2. Unlike in subcritical flows, the thermal boundary condition has a significant effect on the heat transfer behavior in the sCO_2 cases considered, up to 46% variation in heat flux and 10% variation in heat transfer coefficient.
3. This is important in heat exchanger design in sCO_2 systems, as high efficiency heat exchange is necessary for high system performance.

REFERENCES

[1] T.L. Bergman, Introduction to Heat Transfer, John Wiley & Sons, 2011.

[2] P.I. Frank, P.D. David, Introduction to Heat Transfer, John Wiley and Sons, New

Jersey, 1996.

[3] C. Dang, E. Hihara, 2004, In-pipe cooling heat transfer of supercritical carbon dioxide.

Part 1. Experimental measurement, Int. J. Refrig. 27, 736–747.

[4] Y. Li, F. Sun, G. Xie, B. Sunden, J. Qin, 2019, Numerical investigation on flow and thermal performance of supercritical CO_2 in horizontal cylindrically concaved tubes, Applied Thermal Engineering, 153, 655-668

[5] X. Wang, M. Xiang, H. Huo, Q. Liu, 2018, Numerical study on nonuniform heat transfer of supercritical pressure carbon dioxide during cooing in horizontal circular tube, Applied Thermal Engineering, 141, 775-787

[6] M. Xiang, J. Guo, X. Huai, X. Cui, 2017, Thermal analysis of supercritical CO_2 in horizontal tubes under cooling condition, J. Supercritical Fluids, 130, 389-398

[7] Y. Chao, N.C. Lopes, M.A. Ricklick, S.K.S Boetcher, 2021, Effect of the heat transfer coefficient reference temperatures on validating numerical models of supercritical CO_2, J. VVUQ, 6 (4)

[8] Lemmon, E., Huber, M., and McLinden, M., NIST Standard Reference Database 23: Reference Fluid Thermodynamic and Transport Properties-REFPROP, Version 9.0, National Institute of Standards and Technology, Standard Reference Data Program, 2012, Gaithersburg, MD.

[9] Span, R., and Wagner, W., A New Equation of States for Carbon Dioxide Covering the Region From the Triple-Point Temperature to 1100 K at Pressure Up to 800 MPa," J. Phys. Chem, 25(6) (1996), pp. 1509–1596.